The low-spin black hole in LMC X-3

The Astrophysical Journal Letters, 793:L29 (5pp), 2014 October 1 doi:10.1088/2041-8205/793/2/L29

THE LOW-SPIN BLACK HOLE IN LMC X-3

James F. Steiner[1,7], Jeffrey E. McClintock[1], Jerome A. Orosz[2], Ronald A. Remillard[3], Charles D. Bailyn[4], Mari Kolehmainen[5], and Odele Straub[6]
[1] Harvard-Smithsonian Center for Astrophysics, 60 Garden Street, Cambridge, MA 02138, USA; jsteiner@cfa.harvard.edu
[2] Department of Astronomy, San Diego State University, 5500 Campanile Drive, San Diego, CA 92182, USA
[3] MIT Kavli Institute for Astrophysics and Space Research, MIT, 70 Vassar Street, Cambridge, MA 02139, USA
[4] Astronomy Department, Yale University, P.O. Box 208101, New Haven, CT 06520, USA
[5] Astrophysics, Department of Physics, University of Oxford, Keble Road, Oxford OX1 3RH, UK
[6] LUTH, Observatoire de Paris, CNRS, Universite Paris Diderot, 5 place Jules Janssen, F-92190 Meudon, France
Received 2014 August 29; accepted 2014 August 29; published 2014 September 12

ABSTRACT

Building upon a new dynamical model for the X-ray binary LMC X-3, we measure the spin of its black hole (BH) primary via the continuum-fitting method. We consider over one thousand thermal-state *Rossi X-ray Timing Explorer* X-ray spectra of LMC X-3. Using a large subset of these spectra, we constrain the spin parameter of the BH to be $a_* = 0.25^{+0.20}_{-0.29}$ (90% confidence). Our estimate of the uncertainty in a_* takes into account a wide range of systematic errors. We discuss evidence for a correlation between a BH's spin and the complexity of its X-ray spectrum.

Key words: accretion, accretion disks – black hole physics – stars: individual (LMC X-3) – X-rays: binaries

Online-only material: color figure

1. INTRODUCTION

Leong et al. (1971) discovered LMC X-3 during the first year of the *Uhuru* mission. In 1983, Cowley et al. (1983) showed via dynamical observations that the compact X-ray source in this 1.7 day binary is a black hole (BH). In Orosz et al. (2014) we use new optical data to derive a much improved dynamical model of the system. Of chief importance, Orosz et al. report tight constraints on the orbital inclination angle of the binary, $i = 69.^{\circ}2 \pm 0.^{\circ}7$, and the mass of the BH, $M = 7.0 \pm 0.6\,M_{\odot}$.

LMC X-3 is unusual compared to the full assemblage of BH binaries. On the one hand, like the transient systems, its X-ray intensity is highly variable because the BH is fed by Roche-lobe overflow. On the other hand, however, the system almost continually maintains itself in an X-ray bright mode like the persistent (wind-fed) systems (McClintock et al. 2014; Gou et al. 2009; Soria et al. 2001).

Transient versus persistent BHs are further set apart by the properties of their BH primaries: the transient BH masses are low and tightly distributed ($7.8\,M_{\odot} \pm 1.2\,M_{\odot}$), while the masses of the persistent BHs are appreciably higher ($\gtrsim 11\,M_{\odot}$; Özel et al. 2010). Meanwhile, the spins of the transients are widely distributed ($a_* \approx 0$–1), while the three persistent BHs with spin measurements are all high ($a_* \gtrsim 0.85$).

Despite strong variations in X-ray brightness (>3 orders of magnitude), the X-ray spectrum of LMC X-3 is nearly always in a thermal, disk-dominated state (ideal for measuring spin via the continuum-fitting method), except during occasional prolonged excursions into a low-intensity hard state (e.g., Smale & Boyd 2012; Wilms et al. 2001). Because the X-ray spectrum is strongly disk-dominated, relatively featureless, and minimally affected by interstellar absorption, LMC X-3 is a touchstone for testing models of BH accretion disks (e.g., Kubota et al. 2010; Straub et al. 2011; Steiner et al. 2014). In a precursor to this work, we fitted all flux-calibrated archival X-ray spectra to a relativistic accretion-disk model. For hundreds of *Rossi X-ray Timing Explorer* (*RXTE*) spectra, we showed that the inner radius of the disk is constant to within ≈2% over a span of at least 14 yr. Furthermore, for an ensemble of eight X-ray missions spanning 26 yr, we demonstrated the constancy of this radius to better than ≈6%, despite uncertainties associated with cross-calibrating the various detectors and gross variability in the source. This result is the strongest observational evidence that spin can be reliably inferred by measuring the inner-disk radius.

The elegant simplicity of a BH is encapsulated in the famous "no-hair theorem," which tells us that an astrophysical BH is *completely* described by just its mass and spin angular momentum (the third parameter, electrical charge, being effectively neutral in astrophysical settings). A spinning BH is an enormous repository of angular momentum, with the spin as a ready energy source that can be tapped mechanically in a BH's ergosphere. Spin has long been proposed as the likely energy source behind the enormously energetic jets emitted from BHs (e.g., Blandford & Znajek 1977). This assumption has gained recent support both theoretically (e.g., Tchekhovskoy et al. 2011) and observationally (Narayan & McClintock 2012; Steiner et al. 2013; McClintock et al. 2014, but see Russell et al. 2013).

The two primary means by which BH spins are measured are (1) X-ray continuum-fitting (Zhang et al. 1997) and (2) modeling relativistic reflection (frequently termed the "Fe-line" method; Fabian et al. 1989). The single precept that underpins both methods is the monotonic relationship between spin and the radius of the innermost stable circular orbit (ISCO) for particles orbiting the BH. Consequently, by determining $R_{\rm ISCO}$, which is presumed to be the inner radius of the accretion disk, one may directly infer a BH's angular momentum, J, usually expressed as the dimensionless spin parameter,

$$a_* \equiv cJ/GM^2, \quad 0 \leqslant |a_*| \leqslant 1. \tag{1}$$

The continuum-fitting method, which is the basis for this work, has been used to estimate roughly a dozen stellar-mass BH spins (e.g., McClintock et al. 2014, and references therein,

[7] Hubble Fellow.

Middleton et al. 2006; Kolehmainen et al. 2011). In this method, the inner-disk radius is estimated using the thermal, multicolor blackbody continuum emission from the disk (e.g., Novikov & Thorne 1973; Shakura & Sunyaev 1973). The Fe-line method measures $R_{\rm in}$ using the redward extent of relativistic broadening of reflection features in the disk, and has been applied just as widely (e.g., Brenneman & Reynolds 2006; Walton et al. 2012; Reis et al. 2013; Reynolds 2014, and references therein). Both methods, but especially the Fe-line method, are also being applied to measure the spins of supermassive BHs in active galactic nuclei. LMC X-3 is ideal for continuum-fitting as it offers a strong, dominantly thermal continuum at nearly all times. However, its spectra accordingly contain very little signal in reflection and so reflection models cannot constrain spin for this source.

Prior to this investigation, a preliminary estimate of LMC X-3's spin was obtained via a continuum-fitting measurement from a single *BeppoSAX* spectrum by Davis et al. (2006), later bolstered by Kubota et al. (2010). Their results were hampered primarily by the poorly constrained mass available at the time, and so only a rough estimate was possible, $a_* \sim 0.3$. Employing the new and precise mass measurement from Orosz et al. (2014), we revisit LMC X-3's spin determination. Using the largest data set available to us—over a decade of pointed monitoring with (*RXTE*)—and adopting a distance $D = 48.1 \pm 2.2$ kpc (Orosz et al. 2009, 2007),[8] we estimate the spin and its uncertainty for LMC X-3 via X-ray continuum fitting.

2. DATA AND ANALYSIS

We adopt the reduction and analysis techniques used by Steiner et al. (2010) while considering the *full* set of *RXTE* pointed observations over the mission lifetime. To ensure the most consistent analysis, we only use "Standard-2" data collected for the PCU-2 detector, which has the most stable calibration and was most frequently active. We separate and analyze each segment of continuous exposure, applying a 300 s lower limit. For very long observations, we divide the interval into segments with individual exposure times less than 5000 s.[9] In total, this yields 1598 spectra with an average exposure time and signal of $\sim$2 ks and $\sim 50 \times 10^3$ counts, respectively. Background spectra were obtained using the tool pcabackest and subtracted from the data. A correction for the detector dead time ($\sim$1%) has been applied as a model renormalization.[10]

In fitting the spectra, we ignore any channels with energies below (and including) 2.51 keV and above 25 keV. Over the mission lifetime, this corresponds to an evolving range of channels, but always one that is reliably calibrated. We include a 1% systematic error in each channel to account for uncertainties in the response of the detector. Absolute flux calibration is established using the average PCU-2 spectrum of the Crab (Toor & Seward 1974).[11] For this step, we use the model CRABCOR (Steiner et al. 2010) which rescales the normalization by 9.7% and adjusts the spectral index by $\Delta\Gamma = 0.01$. There is relatively little interstellar absorption, $N_{\rm H} = 4 \times 10^{20}{\rm cm}^{-2}$ (Page et al. 2003), which is kept fixed during fitting[12] and modeled via TBABS (Wilms et al. 2000).

Errors are quoted at the 1σ level unless otherwise indicated. For the primary, i.e., thermal disk, component of emission, we use KERRBB2 (McClintock et al. 2014; Davis & Hubeny 2006; Li et al. 2005), which incorporates all relativistic effects and directly solves for spin. The model KERRBB2 assumes that the disk is razor thin and optically thick. To apply KERRBB2 one must specify four external input parameters: BH mass, disk inclination, distance D, and the viscosity parameter α (Shakura & Sunyaev 1973). The Compton power-law component is modeled empirically using SIMPL (Steiner et al. 2009b). Our complete spectral model is expressed as TBABS$\times$(SIMPL$\otimes$KERRBB2)$\times$CRABCOR.

As an initial step in the analysis, we fit the full data set to our spectral model using fiducial values for M, i, and D (Section 1) and adopting a viscosity $\alpha = 0.03$. We include limb darkening and returning radiation effects, adopt zero torque at the inner-disk boundary, and make the standard assumption that the BH's spin axis is aligned with the orbital angular momentum (Steiner & McClintock 2012; McClintock et al. 2014). There are just four free fit parameters: a_*, mass accretion rate $\dot{M}$, photon spectral index Γ, and the scattering fraction $f_{\rm SC}$ (the fraction of disk photons scattered in the corona). We constrain the photon index to lie in the range $\Gamma = 1.5$–3.5; the three other parameters are unconstrained.

Subsequent to fitting all of the spectra, we use our initial results to screen out spectra that are unsuitable for the measurement of spin: We reject data for which $f_{\rm SC}$ exceeds 25% (134/1598; see Steiner et al. 2009a), or for which the goodness-of-fit $\chi^2_\nu > 2$ (4/1598), arriving at a sample of 1461 thermal-state spectra.

As described in Steiner et al. (2010), a large number of LMC X-3's spectra have such a weak power-law component that the spectral index is essentially unconstrained. Roughly half of the sample pegged at a hard limit for Γ while fitting. In a separate analysis with the index fixed at $\Gamma = 2.35$, we have verified that the values of spin returned by these fits are insensitive to whether Γ is fixed or free, and thus pegged fits are deemed reliable and included in our analysis.

Figure 1 shows a fit to one representative spectrum, with the thermal component in red plainly dominant. For this spectrum, our model of a featureless Comptonized disk provides an overconstrained fit, $\chi^2_\nu \approx 0.5$, while the typical goodness-of-fit for this initial run is $\chi^2_\nu \approx 0.7$. Repeating these fits without including the 1% systematic uncertainty produces comparably low values of χ^2_ν.

A restriction of KERRBB2 is that it is only applicable to those data firmly in the "thin-disk" limit (scale height $H/R \ll 1$). The scale-height of the X-ray-emitting region of the disk is determined by radiation pressure, a function of the luminosity. Previous work has demonstrated that a geometrically thin, optically thick disk model is reliable across luminosities $L \approx 5\%$–$30\% L_{\rm Edd}$, where the Eddington luminosity $L_{\rm Edd} \approx 1.3 \times 10^{38}(M/M_\odot)$ erg s^{-1} (McClintock et al. 2014).

3. RESULTS

From our initial run, a total of 410 spectra fulfilling the thermal selection also match this luminosity (thin-disk)

[8] Although LMC X-3 is $\sim 6^\circ$ from the center of the LMC, its distance relative to the center is within our 1σ (2.2 kpc) error because the LMC is viewed nearly face on (Subramanian & Subramaniam 2013).

[9] An alternate analysis without subdividing the long observations produces identical results.

[10] The correction has been estimated based on the normal and "very long" event rates, in the manner detailed in McClintock et al. (2006).

[11] We have explored the variability of the Crab's spectrum (Wilson-Hodge et al. 2011) on our results and find that it has negligible impact on the spin measurement.

[12] As shown in Steiner et al. (2010, their Figure 3), uncertainty in $N_{\rm H}$ has no bearing on the *RXTE* fits to this source.

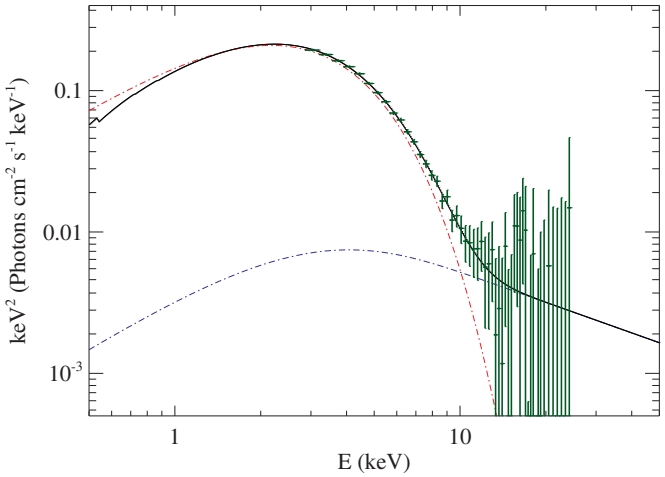

Figure 1. Representative fit to a 4 ks exposure of LMC X-3 from 1998 December 9. The black line shows the composite model, including photoelectric absorption. The red and blue dash-dotted lines show the intrinsic thermal disk and power-law components, respectively.

(A color version of this figure is available in the online journal.)

criterion. This subsample shows the same low goodness of fit ($\chi^2/\nu \approx 0.7$). Using those spectra that make both cuts, we obtain a spin $a_* = 0.205 \pm 0.004$ (weighted mean and its 1σ error, computed including sample variance).

A comprehensive run is now performed to assess the error in spin from uncertainties in the other measurement quantities. For each point along a grid of M, i, and D ($25\times21\times16$ grid elements), we repeat our spectral fits to the pre-selection of 1454 spectra. Mass is sampled from M: 5–11 $M_\odot$, inclination i: 60°–75°, and D : 41–56 kpc. The values of $L/L_{\rm Edd}$ depend upon M, i, and D, but typically ~400 thermal spectra fulfill the luminosity criterion. At *each* gridpoint, the distribution of spin produces a weighted mean and its uncertainty.[13] By applying weights according to the probability of each gridpoint (weighted according to the measurements of M, i, and D given in Sections 1 and 2), individual results are combined to achieve a composite distribution in spin. This distribution is inclusive of *all measurement errors*. The several percent uncertainty for each point in the grid is largely set by the data scatter, which reflects the slight correlation between spin (inner radius) and luminosity. This correlation is discussed for LMC X-3 in Steiner et al. (2010) and illustrated there in Figure 2.

In previous work, we have assessed the effects of a wide range of systematic errors (Steiner et al. 2010, 2011) and found that only two are significant: the uncertainty in α and the uncertainty in the spectrum of the Crab, which we use as our flux standard (Section 2). Unlike other parameters of the disk model, we cannot fit for α. Instead, we take its uncertainty into account by performing the analysis for $\alpha = 0.01$ and $\alpha = 0.1$ and then averaging the spin distributions, weighting them equally. We incorporate a 10% uncertainty in the absolute X-ray flux calibration (Toor & Seward 1974) by broadening our distribution in $R_{\rm in}$ using a Gaussian kernel with 5% width. Finally, an additional 2% broadening is used to account for the small variation introduced by adopting a different choice of Comptonization model (Steiner et al. 2010).

[13] As demonstrated in Steiner et al. (2010), the inner disk radius (which corresponds to a particular value of spin) at any grid point has a spread of <5%, while the mean of the distribution is determined with much greater precision even here as we account for sample variance in the weighted error.

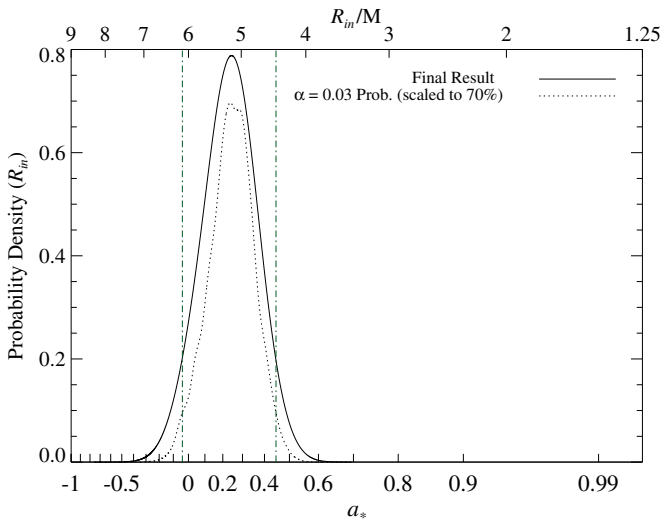

Figure 2. Net probability distribution of a_* ($R_{\rm in}$). The abscissa is scaled logarithmically in $R_{\rm in}$, our observable. The corresponding quantity of chief physical interest, a_*, is shown on the lower axis. Our final distribution (solid line) incorporates measurement and systematic errors, including uncertainties in the α viscosity and absolute flux calibration. Dash-dotted lines indicate the 90% confidence interval. A dotted line shows the result for $\alpha = 0.03$ ignoring systematic error (where the probability distribution has been rescaled for comparison).

Table 1
Spin Determination

Confidence Level	Spin Interval ($a_* =$)	$R_{\rm in}$ Interval ($R_{\rm in}/M =$)
68% (1σ)	$0.25^{+0.13}_{-0.16}$	5.2 ± 0.5
90%	$0.25^{+0.20}_{-0.29}$	$5.2^{+1.0}_{-0.7}$
95% (2σ)	$0.25^{+0.24}_{-0.36}$	$5.2^{+1.2}_{-0.9}$
99.7% (3σ)	$0.25^{+0.32}_{-0.55}$	$5.2^{+1.8}_{-1.2}$

Note. Incremental confidence intervals for our final, adopted spin result, accounting for all sources of error.

The combined result is shown in Figure 2. Our *final* measurement of spin, including all measurement *and* systematic uncertainties is $a_* = 0.25^{+0.20}_{-0.29}$ (90%). For comparison, our measurement without considering systematic errors (for $\alpha = 0.03$) yielded $a_* = 0.24^{+0.16}_{-0.23}$ (90%). Table 1 gives our final determination of spin as measured at several confidence levels.

As a bottom line, LMC X-3 has a precisely determined spin, which is low.

4. DISCUSSION

In Section 3 we considered measurement errors and known systematic uncertainties (apart from the assumption that the BH's spin is aligned with the orbital angular momentum vector; see Section 5.4 in McClintock et al. 2014). In this section we consider error that we incur due to our reliance on the Novikov–Thorne model and conclude that it is minor. We then compare the low spin of LMC X-3 to the spins of several other sources, tentatively concluding that the Compton component is characteristically weak for low spin BHs and strong for rapidly spinning ones.

4.1. Errors from the Novikov–Thorne Model

While our earlier study of LMC X-3 (Steiner et al. 2010), and similar studies of other BH binaries (e.g., Gierliński & Done

2004), provide compelling evidence that the inner disk radius is constant in BH binaries, it does not establish whether or not $R_{\rm in}$ matches $R_{\rm ISCO}$. The central assumption of the thin-disk model is that the viscous torque vanishes at the ISCO and that no flux is emitted from within the inner radius. This assumption has been tested by several groups using sophisticated general-relativistic magnetohydrodynamic codes. The results from two groups are exemplified by three key studies, each aimed at testing the reliability of spin estimates. Results from one group are reported in Noble et al. (2011) and from the other in Kulkarni et al. (2011) and Zhu et al. (2012). Both groups produce synthetic observations of their simulations as they would appear to a distant observer at a range of viewing angles.

Although there are subtle differences in the approaches taken by the two groups, one can make a reasonably direct comparison between Kulkarni et al. (2011) and Noble et al. (2011). Both groups used ad hoc but reasonable cooling prescriptions in post-processing to convert magnetic stresses into radiation. By treating the dissipation as local and thermal, disk spectra have been generated for a nonspinning BH by Noble et al. and for BHs with a range of spins by Kulkarni et al. From these two works, one concludes that spin is systematically *overestimated*, that this effect is most pronounced at high inclination, and that the fractional change in $R_{\rm in}$ is independent of a_*. The deviation of $R_{\rm in}/R_{\rm ISCO}$ from unity is of the order of 10%. However, a state-of-the-art analysis has been achieved by Zhu et al. (2012) and their findings differ appreciably from those of others, as we now discuss.

Zhu et al. compute (in post-processing) full radiative transfer through the disk atmosphere. In contrast to the $\sim$10% shift in $R_{\rm in}/R_{\rm ISCO}$ reported by Kulkarni et al. (2011) and Noble et al. (2011), Zhu et al. find a much smaller deviation because their more sophisticated approach identifies a hard power-law component of emission originating from inside $R_{\rm ISCO}$. It is this component, which, in the earlier work, was lumped in with the thermal emission, that was largely responsible for the shift in $R_{\rm in}/R_{\rm ISCO}$. Analyzing their simulated spectra using the model in Section 2, Zhu et al. find that the shift in $R_{\rm in}/R_{\rm ISCO}$ is only $\sim 3\% \pm 2\%$ and that it depends only weakly on inclination, α, and luminosity (see Table 2 in Zhu et al. 2012).

In short, deviations from Novikov–Thorne are likely of minor consequence. For the nominal spin of LMC X-3, a 3% offset in $R_{\rm in}$ would imply $a_* \approx 0.20$ (a shift of $\Delta a_* = -0.05$), or a $\sim 0.3\sigma$ correction to our final result.

4.2. A Possible Link Between Spin and Spectral Complexity

Although the spins of over a dozen stellar-mass BHs have been measured, only two sources have spins that are small comparable to that of LMC X-3, namely, A0620–00 and H1743–322 (McClintock et al. 2014). The thermal spectra of these BHs, especially A0620–00 and LMC X-3, are remarkably simple, consisting of a dominant thermal component with a Compton power-law and reflection components that are always quite faint.

By contrast, the two sources that have been confirmed to have extreme spins, Cyg X–1 and GRS 1915+105 (McClintock et al. 2014), exhibit strong Comptonization, strong reflection, and strong rms variability (from their power-density spectra). On this basis, we tentatively suggest a correlation between spectral complexity and spin.

If true, we then predict that the spin of GS 2000+25 should be low (see Terada et al. 2002), and the spin of V404 Cyg should be high (see Tanaka & Lewin 1995). We suggest 4U1957+11 as another useful test source. Although its spin and mass are presently unknown, there are indications that the former is likely very high and the latter is likely low (Nowak et al. 2012). At the same time, its spectrum is simple and thermal with very weak Comptonization/reflection. Confirmation of an extreme spin for 4U1957+11 could decisively rule out this hypothesis.

5. CONCLUSIONS

We have analyzed all 1598 spectra of LMC X-3 collected during the *RXTE* mission. Using a selected sample of $\approx$400 spectra, recent precise measurements of BH mass and inclination (Orosz et al. 2014), and employing continuum fitting, we derive a strong constraint on the BH's spin: $a_* = 0.25^{+0.20}_{-0.29}$ (90% confidence). Our comprehensive error estimate takes into account all known sources of uncertainty, e.g., uncertainties in M, i, D, α, and in the absolute X-ray flux calibration.

The simple and predominately thermal spectra of LMC X-3 and A0620–00, the BHs with the smallest measured spins, contrast sharply with the complex and strongly Comptonized spectra of GRS 1915+105 and Cyg X–1, two BHs with near-extreme spin. This suggests a possible link between spin and the degree of spectral complexity, a hypothesis that can be tested, and which predicts a low spin for GS 2000+25 and a high spin for V404 Cyg. The BH 4U 1957+11 may allow a falsification of the hypothesis if its spin can be verified.

By virtue of the no-hair theorem, we have a complete and quite precise description of the BH in LMC X-3. These three—and only three— characteristics define the BH in its entirety: zero charge, $M \approx 7.0\,M_\odot$, and $a_* \approx 0.25$.

We thank Chris Done and Lijun Gou for enlivening discussions, the anonymous referee, and Colleen Hodge-Wilson for providing data on the Crab's variability. Support for J.E.M. has been provided by NASA grant NNX11AD08G and support for J.F.S. by NASA Hubble Fellowship grant HST-HF-51315.01.

Facility: RXTE

REFERENCES

Blandford, R. D., & Znajek, R. L. 1977, MNRAS, 179, 433
Brenneman, L. W., & Reynolds, C. S. 2006, ApJ, 652, 1028
Cowley, A. P., Crampton, D., Hutchings, J. B., Remillard, R., & Penfold, J. E. 1983, ApJ, 272, 118
Davis, S. W., Done, C., & Blaes, O. M. 2006, ApJ, 647, 525
Davis, S. W., & Hubeny, I. 2006, ApJS, 164, 530
Fabian, A. C., Rees, M. J., Stella, L., & White, N. E. 1989, MNRAS, 238, 729
Gierliński, M., & Done, C. 2004, MNRAS, 349, L7
Gou, L. J., McClintock, J. E., Liu, J., et al. 2009, ApJ, 701, 1076
Kolehmainen, M., Done, C., & Díaz Trigo, M. 2011, MNRAS, 416, 311
Kubota, A., Done, C., Davis, S. W., et al. 2010, ApJ, 714, 860
Kulkarni, A. K., Penna, R. F., Shcherbakov, R. V., et al. 2011, MNRAS, 414, 1183
Leong, C., Kellogg, E., Gursky, H., Tananbaum, H., & Giacconi, R. 1971, ApJL, 170, L67
Li, L.-X., Zimmerman, E. R., Narayan, R., & McClintock, J. E. 2005, ApJS, 157, 335
McClintock, J. E., Narayan, R., & Steiner, J. F. 2014, SSRv, 183, 295
McClintock, J. E., Shafee, R., Narayan, R., et al. 2006, ApJ, 652, 518
Middleton, M., Done, C., Gierliński, M., & Davis, S. W. 2006, MNRAS, 373, 1004
Narayan, R., & McClintock, J. E. 2012, MNRAS, 419, L69
Noble, S. C., Krolik, J. H., Schnittman, J. D., & Hawley, J. F. 2011, ApJ, 743, 115
Novikov, I. D., & Thorne, K. S. 1973, in Black Holes, ed. C. DeWitt & B. DeWitt (Paris: Gordon & Breach), 343
Nowak, M. A., Wilms, J., Pottschmidt, K., et al. 2012, ApJ, 744, 107
Orosz, J. A., McClintock, J. E., Narayan, R., et al. 2007, Natur, 449, 872
Orosz, J. A., Steeghs, D., McClintock, J. E., et al. 2009, ApJ, 697, 573

Orosz, J. A., Steiner, J. F., McClintock, J. E., et al. 2014, ApJ, in press (arXiv:1402.0085)
Özel, F., Psaltis, D., Narayan, R., & McClintock, J. E. 2010, ApJ, 725, 1918
Page, M. J., Soria, R., Wu, K., et al. 2003, MNRAS, 345, 639
Reis, R. C., Reynolds, M. T., Miller, J. M., et al. 2013, ApJ, 778, 155
Reynolds, C. S. 2014, SSRv, 183, 277
Russell, D. M., Gallo, E., & Fender, R. P. 2013, MNRAS, 431, 405
Shakura, N. I., & Sunyaev, R. A. 1973, A&A, 24, 337
Smale, A. P., & Boyd, P. T. 2012, ApJ, 756, 146
Soria, R., Wu, K., Page, M. J., & Sakelliou, I. 2001, A&A, 365, L273
Steiner, J. F., & McClintock, J. E. 2012, ApJ, 745, 136
Steiner, J. F., McClintock, J. E., & Narayan, R. 2013, ApJ, 762, 104
Steiner, J. F., McClintock, J. E., Orosz, J. A., et al. 2014, ApJ, 783, 101
Steiner, J. F., McClintock, J. E., Remillard, R. A., et al. 2010, ApJL, 718, L117
Steiner, J. F., McClintock, J. E., Remillard, R. A., Narayan, R., & Gou, L. J. 2009a, ApJL, 701, L83
Steiner, J. F., Narayan, R., McClintock, J. E., & Ebisawa, K. 2009b, PASP, 121, 1279
Steiner, J. F., Reis, R. C., McClintock, J. E., et al. 2011, MNRAS, 416, 941
Straub, O., Bursa, M., Sądowski, A., et al. 2011, A&A, 533, A67
Subramanian, S., & Subramaniam, A. 2013, A&A, 552, A144
Tanaka, Y., & Lewin, W. H. G. 1995, in X-ray Binaries, ed. W. H. G. Lewin, J. van Paradijs, & E. P. J. van den Heuvel (Cambridge: Cambridge Univ. Press), 126
Tchekhovskoy, A., Narayan, R., & McKinney, J. C. 2011, MNRAS, 418, L79
Terada, K., Kitamoto, S., Negoro, H., & Iga, S. 2002, PASJ, 54, 609
Toor, A., & Seward, F. D. 1974, AJ, 79, 995
Walton, D. J., Reis, R. C., Cackett, E. M., Fabian, A. C., & Miller, J. M. 2012, MNRAS, 422, 2510
Wilms, J., Allen, A., & McCray, R. 2000, ApJ, 542, 914
Wilms, J., Nowak, M. A., Pottschmidt, K., et al. 2001, MNRAS, 320, 327
Wilson-Hodge, C. A., Cherry, M. L., Case, G. L., et al. 2011, ApJL, 727, L40
Zhang, S. N., Cui, W., & Chen, W. 1997, ApJL, 482, L155
Zhu, Y., Davis, S. W., Narayan, R., et al. 2012, MNRAS, 424, 2504